View metadata, citation and similar papers at core.ac.uk
brought to you by CORE
provided by CSCanada.net: E-Journals (Canadian Academy of Oriental and Occidental Culture,...

ADVANCES IN PETROLEUM EXPLORATION AND DEVELOPMENT
Vol. **1**, No. **1**, **2011 PP. 1-13**
ISSN 1925-542X[PRINT]
ISSN 1925-5438[ONLINE]

CSCanada
www.cscanada.net
www.cscanada.org

Hydrocarbon Formation in Immature Sediments

D.D.J. ANTIA[1,*]

[1]DCA Consultants Ltd., Haughend Farm, Bridge of Earn Road, Dunning, Perthshire, PH2 9BX. UK

* Corresponding author. Email: dcacl@btconnect.com

Abstract: Immature sediments (R_o=<0.6) and hydrates commonly contain low concentrations of C_{2-8+} alkanes/alkenes, higher alkanes, cycloalkanes and aromatics (temperature=<373 K; Pressure=<100 MPa). Their origin is enigmatic. Traditionally they are interpreted as migrated thermogenic oil. Water treatment experiments have established that they could be formed through the interaction of water and organic carbon by Fe catalysis at 298 K. This study investigates the Eh and pH associated with low temperature (263-298 K) hydrocarbon formation in saline pore-waters containing Ca-montmorillonite and Fe^0 (ZVI) over a 300 day period in order to identify the principal reaction mechanisms. The interaction of flowing gaseous carbon dioxide-hydrocarbon mixtures with halite promoted with Fe_xO_y, $Fe_x[OH]_y$ at 288 – 308 K is examined experimentally. The study established that halite and mixtures of halite with organic material, Fe-montmorillonite, $CaCO_3$, $Ca(OH)_2$, $MgSO_4$, $(NH_4)_2SO_4$, K_2SO_4, pyroclastics, ash, phosphate enriched organic material, and coal can facilitate the removal of CO_2, the formation of H_2O on the catalyst surface, and the formation of hydrocarbons incorporating the CO_2.

Key words: ZVI; Oil formation; CO_2; Eh; pH; NaCl; Halite; Montmorillonite

1. INTRODUCTION

Some light hydrocarbons (C_{2+}) found in immature sediments (R_o = <0.6) and with methane hydrates (temperature = <373 K; Pressure = <100 MPa; 0-500 mbsb) from the Lower Congo Basin (East Atlantic), West Pacific Continental Slope, Pacific Abyssal Plain, and Indian Ocean Abyssal Plain may have been formed in situ by catalysis within the pore-waters (Antia, 2008a; 2009a; 2009b).

The principal catalytic processes for hydrocarbon formation are:

a. ***Sabatier Process*** (also known as the Fischer Tropsch (FT) Process (e.g. Elworthy & Williamson, 1902; Sabatier, 1908; 1910; Storch *et al.* 1951; Steynberg & Dry, 2004)) where $aCO + bH_2 = C_xH_y + cH_2O + dCO_2$ (alkanes and alkenes (gas + oil)). Variants include $aCO + bH_2 + C_xH_y = C_{x+n}H_{y+m} + cH_2O + dCO_2$. By-products include $C_xH_yO_z$. This process requires a gaseous reaction environment (423-673 K, 0.1 – 5 MPa).

b. ***Kolbel-Engelhardt (KE) Process*** (e.g. Kolbel & Englehardt, 1959; O'Rear, 2005) where $3nCO+nH_2O = C_nH_{2n}+2nCO_2$ and $nCO_2 +3nH_2 = C_nH_{2n} +2nH_2O$. i.e. $mCO_2 + 3nCO + nH_2O + 3mH_2 = C_{(n+m)}H_{2(n+m)}+2mH_2O +2nCO_2$.This process requires a gaseous reaction environment (423-673 K, 0.1 – 5 MPa).

c. ***Polymerisation Process*** (e.g. Baxendale *et al.* 1946a; 1946b; 1946c; Hori *et al.* 1989; Hardy & Gillham, 1995; Campbell *et al.* 1997; Deng *et al.* 1997;1999; Schrick *et al.* 2002; Lim *et al.* 2007; Antia, 2008a; 2009a; 2009b; 2010; 2011; Bokare & Choi, 2009) where hydrocarbons form catalytically in an aqueous environment from the reductive/oxidative interaction and polymerisation of $H_xC_yO_z$, C_xH_y, C_x, CO_x, H_xO_y, organo-halides and metal carbonyls/carbides.For example 74.7 API Lower Congo Basin oil found in association with methane hydrates in methane vents (pockmarks), may have been formed (Antia, 2008a) by the generic equation 4.09 m^3 CH_4 + 3.09 m^3 CO_2 + 6.18 m^3 H_2= 4.96 kg H_2O + 4.58 kg Oil [where 3.09 CO_2 + 6.18 H_2 = 3.09 HCO + 3.09 H_3O^+ = 3.09

†Received 2 May 2011; accepted 8 June 2011. **DOI:** 10.3968/j.aped.1925543820110101.001

H_2CO [formaldehyde] + 3.09 H_2O].This process requires an aqueous reaction environment (<260->373 K, <0.1 – >80 MPa).

The FT and KE processes are unlikely to be responsible for the formation of low temperature hydrocarbons (Storch *et al.* 1951; Steynberg & Dry, 2004). Experiments (Deng *et al.* 1997) have established that C_{2+} hydrocarbons can be formed over short time interval at 298 K using a carbon source (C, or metal carbide, or CH_4) + an oxidant source (H_2O or CO_2).

This study uses two experiments to establish the mechanism for aqueous phase hydrocarbon chain growth utilising Fe catalyst + H_2O [the oxidant] + C [the carbon source] (Experiment I) and for gaseous phase hydrocarbon chain growth utilising NaCl catalysts + CO_2 (the oxidant) + CH_4 [the carbon source] (Experiment II) at temperatures of 260 – 308 K. Both reaction routes may be present in the immature sediments of the continental slope and abyssal plain.

2. CHEMICAL BACKGROUND

In the geological environment, products and reactants are present as solids, liquids, gases and supercritical fluids. These phases affect the heat of formation (and reaction) [ΔH], the Gibbs free energy [ΔG], the equilibrium constants, the reaction rates and the availability of intermediate reaction routes.

a. ***Heats of Formation*** change with product or reactant phase. The Heat of Reaction [ΔH_R] = ΣΔH(Products) -ΣΔH(Reactants) (Kotz & Treichel, 1996). Reactions with a negative ΔH_R (exothermic) are likely to progress at low temperatures.

b. ***Gibbs Free Energy*** ΔG = ΣΔG(Products) -ΣΔG(Reactants) (Kotz & Treichel, 1996). The equilibrium constant (K_r) defines the extent to which a reaction occurs at a specific temperature (T, K). i.e. $\Delta G\ (T) = -RT \ln[K_r(T)]$; R = gas constant. Endothermic reactions become more thermodynamically favourable at higher temperatures as $\ln[(K_r(T_2))/(K_r(T_1))] = \Delta H_R/R[(1/T_2)-(1/T_1)]$. ΔG changes with product or reactant phase. Reactions with a negative ΔG are spontaneous.

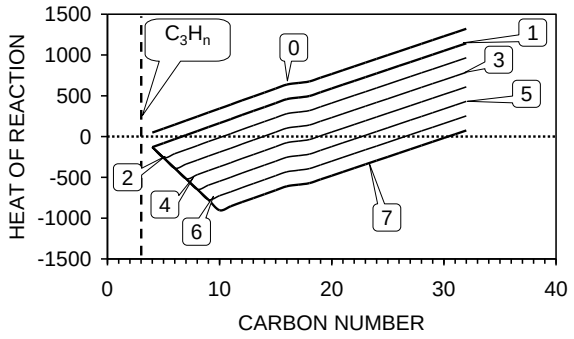

Fig. 1: Heat of Reaction (kJ mol^{-1} product alkane)

Chain growth is from an alkane/alkene nucleus and occurs by adding aCH₄ + bCO₂, where b varies between 0 and 7, and a = n-m-b; n = number of carbon atoms in the finished n-alkane; m = number of carbon atoms in the starting alkane. m for C_3H_8 = 3.

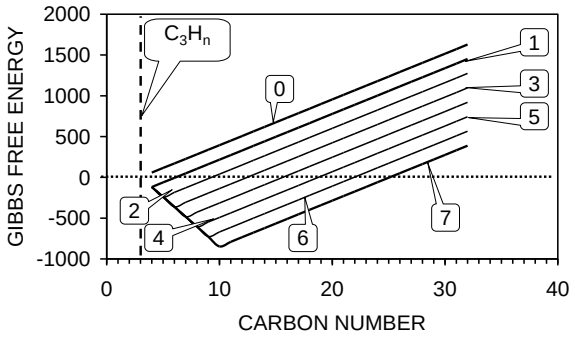

Fig. 2: Gibbs Free Energy(kJ mol^{-1} product alkane)

For n-alkanes where chain growth by accretion is from an alkane/alkene nucleus and accretion occurs by adding aCH₄ + bCO₂. See Fig.1 caption for key.

In this study, [ΔH, ΔH_R, ΔG] are referenced to T = 298.15K, pressure, P= 0.1 MPa. ΔH, ΔH_R, ΔG vary with temperature. K_r varies with T and P and can be approximated (Antia, 2009b) as:$K_p/K_c = (R\ P_{at}\ T)^c$; P_{at} = pressure (atmospheres); c= moles gaseous reactants – moles gaseous products; K_c = equilibrium constant at STP, K_p = equilibrium constant at P and T.

2.1 Low Temperature Thermodynamics

Reactions involving CO_2 and H_2(at 423- 573 K, 0 – 5 MPa) are interpreted (Kuster, 1936a; 1936b; Puskas, 1997) as a two-stage Fischer Tropsch (FT) reaction where Stage 1 hydrogenates CO_2. i.e. $CO_2 + H_2 = CO + H_2O$ (g) $H_R^{298.15K}$ = 41.2 kJ mol^{-1}; $CO_2 + H_2 = CO + H_2O$ (l) $H_R^{298.15K}$ = -2.8 kJ mol^{-1}. The second stage follows a standard FT hydrogenation of CO to form oil. The first stage is exothermic when the H_2O product is maintained as a liquid or supercritical fluid. The thermodynamics for chain growth on a C_3H_8 nucleus by the addition of CO_2 and CH_4(C_3H_8+ $bCO_2 + aCH_4 + bH_2 = C_nH_{2n+2} + cH_2O + dH_2$; n=3+a+b) is both exothermic and spontaneous at T = 298.15K (Fig. 1, 2). The thermodynamics indicate that a mixture of catalyst (e.g. zero valent iron (Fe^0), or Fe_xO_y), water, methane and

CO_x (or H_yCO_x) will result in the formation of hydrocarbons at ambient temperatures and pressures. H_2=H_2(aq, g), $2H_3O^+$ or $2H^+$.

2.2 Formation of Hydrocarbons from Water, Carbon, and Fe^0

Placement of 5gm iron filings (3.09 wt% C; surface area = 1.18 m^2/g) + 15 ml pure H_2O (0.0015 M CO_2 and 0.03M CO_2) in sealed containers at 293 K demonstrate (Fig. 3, 4) a progressive increase in evolved hydrocarbons with time (Deng *et al.* 1997). After 40 days similar levels of ethane to pentane hydrocarbons were present. The methane product concentration was higher when high initial concentrations of dissolved CO_2 (Fig. 3) were present. The overall number of carbon atoms incorporated in hydrocarbon formation increases with increased CO_2 concentration (Fig. 4) and availability of carbon. Carbon incorporation into new alkanes/alkenes follows a linear relationship.

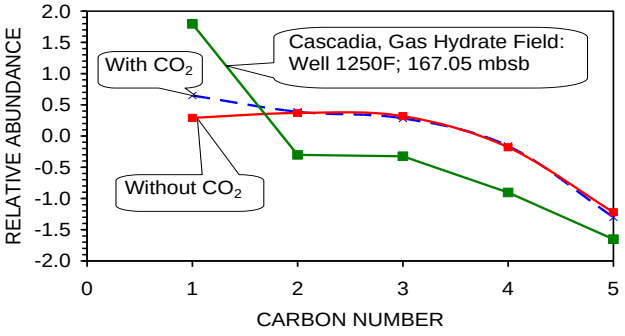

Fig. 3: Iron Catalysed Hydrocarbons

Formed in a sealed reactor (5 g Fe^0 + 15 cm^3 H_2O) at 283 K (in CO_2 (0.0015 M) poor and CO_2 (0.03 M) enriched water) after 40 days. A typical gas sample from the Cascadia hydrate field (263 – 290 K, >9 MPa) shows a similar pattern of relative ethane to pentane molar abundance. The methane yield without CO_2 (0.0015 M) = 8.7 cm^3 kg Fe^0 40 d^{-1}= 282.8 cm^3 kg C 40 d^{-1}; The methane yield with CO_2 (0.03 M) = 20.8 cm^3 kg Fe^0 40 d^{-1}= 674.5 cm^3 kg C 40 d^{-1}; Data Sources: Deng *et al.* 1997; Antia, 2009b.

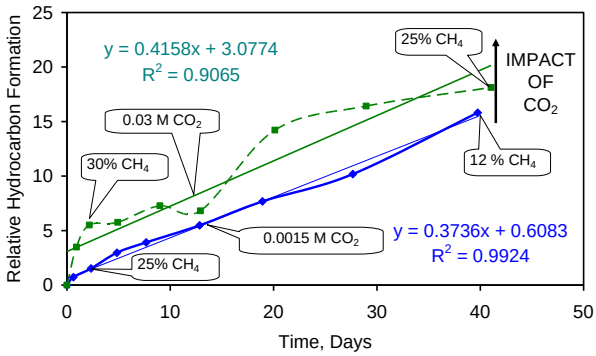

Fig. 4: Iron Catalysed Hydrocarbons

Formed at 283 K (in CO_2 poor and CO_2 enriched water). Data Source: Deng *et al.* 1997. Relative Hydrocarbon Formation = A_1 + $2A_2$ + $3A_3$ + $4A_4$ + $5A_5$. A_1 to A_5 = molar abundance of methane to pentane.

2.3 Interpreted Hydrocarbon Formation Reactions

The interpreted primary oxidative and hydrogenation chain growth reactions (Baxendale *et al*. 1946a; 1946b; Mwebi, 2005; Antia, 2009a;2009b; 2010; 2011; Braun, 2009; Kang & Choi, 2009) are:

$$Fe + H_2O = Fe\text{-}H^+ + OH^- \quad \text{(E1)}$$

[Catalytic nuclei formation, pH increase, Eh decrease]

$$Fe\text{-}H^+ + 2H_2O + C = Fe\text{-}CH_3 + 2OH^- \quad \text{(E2)}$$

[Chain initiation, pH increase, Eh decrease]

Chain growth on a specific site may be associated with an increase in OH^- and a corresponding increase in pH.

$$Fe\text{-}CH_3 + 2H_2O + C = Fe\text{-}CH_2CH_3 + 2OH^- \quad \text{(E3)}$$

[Chain growth, pH increase, Eh decrease]

$$Fe\text{-}CH_3 + 2nH_2O + nC = Fe\text{-}[CH_2]_nCH_3 + 2nOH^- \quad \text{(E4)}$$

[Chain growth, pH increase, Eh decrease]

Alternatively, chain growth is associated with a decrease in OH^- and a corresponding decrease in pH.

$$Fe\text{-}CH_3 + 2OH^- + C = Fe\text{-}CH_2CH_3 + O_2 \quad \text{(E5)}$$

[Chain growth, pH decrease, Eh increase]

$$Fe\text{-}CH_3 + 2nOH^- + nC = Fe\text{-}[CH_2]_nCH_3 + nO_2$$
[Chain growth, pH decrease, Eh increase] (E6)

The O_2 is present as $O_2(g)$, $O_2(aq)$, O_2H^- (aq), $Fe[OH]_x$,Fe_xO_y (Antia, 2010; 2011). Chain cleavage to release the hydrocarbon may take the form:

$$Fe\text{-}CH_3 + 2H_2O = Fe\text{-}H^+ + CH_4 + 2OH^-$$
[Chain cleavage to form methane, pH increase, Eh decrease] (E7)

$$Fe\text{-}CH_3 + 2OH^- = Fe\text{-}H^+ + CH_4 + O_2$$
[Chain cleavage to form methane, pH decrease, Eh increase] (E8)

$$Fe\text{-}[CH_2]_nCH_3 + 2nOH^- = Fe\text{-}H^+ + C_{n+1}H_{2n+4} + nO_2$$
[Chain cleavage to form an alkane, pH decrease, Eh increase] (E9)

$$Fe\text{-}[CH_2]_nCH_3 = Fe\text{-}H^+ + C_{n+1}H_{2n+2}$$
[Chain cleavage to form an alkene, no change in pH or Eh] (E10)

The effect of CO_2 is to reduce the availability of H^+ ions, thereby increasing pH (Deng *et al.* 1997),

$$H_2CO_3\,(aq) + 4Fe(s) + 8H^+ = CH_4 + 4Fe^{2+}(aq) + 3H_2O:$$
$$G = -438.21\ kJmol^{-1} \quad (E11)$$

Consequently sediments containing biogenic activity (or carbonates) can be expected to contain high concentrations of Fe catalysed methane while the relative molar abundance pattern for catalysed ethane to pentane remains unchanged. Similar ethane – pentane molar abundance patterns are present in the Cascadia gas hydrate field (East Pacific continental slope) (Fig. 3).The oxidation-reduction reactions associated with hydrocarbon formation are oscillatory Fenton Reactions (Barbusinsky, 2009; Antia, 2010; 2011). They may also involve an electron shuttle mechanism(Antia, 2010; 2011; Bokare & Choi, 2009; Kang & Choi, 2009).

3. EXPERIMENT Ⅰ

Experiment Ⅰ establishes if the hydrocarbon chain growth and chain termination (E1 to E10) resulting from the interaction of Fe^0 and H_2O is associated with the formation of OH^-, or O_2H, or O_2 or $Fe[OH]_x$ or Fe_xO_y.

3.1 Reactors

a. *Base Case Sealed Static Diffusion Reactor:* 60 g/L Ca-montmorillonite + 90 g/L n-Fe^0 (60-120 K nm) were placed in 0.2 L of 0.96 PSU water. Temperature was maintained between 263 and 298 K for a period of 300 days.

b. *Control Case Sealed Static Diffusion Reactor:* 60 g/L Ca-montmorillonite was placed in 0.2 L of 0.96 PSU water. Temperature was maintained between 263 and 298 K for a period of 300 days.

3.2 Measurements

Measurements were made of Eh, pH, and temperature using Hanna HI-98120 (ORP/Temperature, Hanna Calibration Number = 24230), Hanna HI-98129 (pH, EC, TDS, Temperature; Hanna Calibration Number = 33999). Hi-98120 is factory calibrated. HI-98129 was calibrated using Hanna test reagents (*pH* buffer solutions 4.01, 7.01, 10.01 (HI-7004, HI-7007, HI-7010) and conductivity solution 1.413 mS cm^{-1} (HI-7031)). $Eh_{298.15K}$ calculated from ORP as *Eh* = ORP ($298.15/T_o$) [1]. T_o = measured temperature, K. The evolution of gases (O_2, C_xH_y, H_2) was monitored.

3.3 Eh-pH Changes –Base Case

The initial formation of CH_4, Fe-H^+ and Fe-CH_3 (Fig.3,4) is associated (Fig. 5) with a very significant increase in pH (i.e. ratio of OH^-:H^+). This is associated with a decrease in Eh (i.e. a decrease in the O_2H:OH ratio). These experimental observations are consistent with equations E1, E2 and E7.

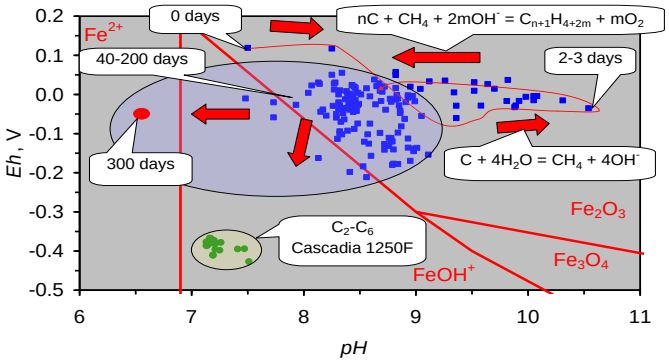

Fig. 5: Iron Catalysed Changes

In water Eh & pH associated with hydrocarbon formation at 255 – 298 K at 0.1 MPa in a sealed static diffusion reactor containing 0.2 L saline H_2O. The Eh & pH of sediments which have been interpreted (Antia, 2009b) as containing in situ ethane to hexane (Cascadia, gas hydrate field (263-290 K), ODP Leg 204, well 1250 F, 155 – 179 mbsb; water depth = 795.4 m) are shown for comparison.

Chain growth and the progressive formation of higher hydrocarbons (Fig. 3, 4) is associated with a decrease in pH and a stable or decreasing Eh (Fig. 5). This indicates consumption of OH^- to reduce pH and a faster consumption of O_2H than OH^- to reduce Eh. These experimental observations suggest that equations E3, E4 only apply to a minor extent, and that E5, E6, E9, and E10 dominate during the formation of higher hydrocarbons. During this phase CH_4 may be formed in accordance with either E7 or E8.

O_2H and OH are relatively unstable ions. The relevant reactions (Barbusinski, 2009; Bokare & Choi, 2009; Kang & Choi, 2009; Antia, 2010) include:-

$$4OH^- = 2H_2O_2 = 2H_2O + O_2(g) \text{ [pH decrease, Eh increase]}$$
$$OH + H_2O_2 = O_2H + H_2O \text{ [Eh increase]} \quad \text{(E12)}$$

$$OH^- + O_2H^- = H_2O + O_2(g) \text{ [Eh increase, pH decrease]}$$
$$Fe^{3+} + O_2H = Fe^{2+} + H^+ + O_2 \text{ [Eh increase, pH decrease]} \quad \text{(E13)}$$

The characteristic deep brown-red iron complexes (Fig. 6a, d) are an ion pair complex (E14) formed (Evans *et al*. 1949; George, 1952; Behar & Stein, 1966) as:-

$$Fe^{3+} + O_2H^- = [FeO_2H]^{2+} \text{ [Eh decrease, pH decrease]} \quad \text{(E14)}$$

The colour due to the hydroxyl reaction (E15) is negligible (Evans et al., 1949):

$$Fe^{3+} + OH^- = [Fe^{3+}OH^-] \text{ [Eh increase, pH decrease]} \quad \text{(E15)}$$

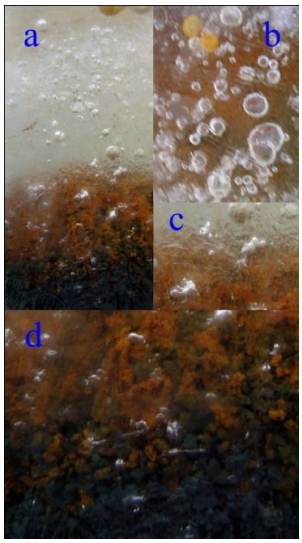

Fig. 6: Iron Catalysed Hydrocarbon and Oxygen Formation

At 273 K at Day 300 (a) Vertical section through the sediment-water interface. O_2 + H_2 + CH_4/C_{1+} degassing from n-Fe^0 (black) through $Fe_2O_3/Fe(OH)_x$ + Ca-montmorillonite to H_2O (s). (b) View from upper surface of water showing Fe_2O_3 /$Fe(OH)_x$ (principally $[FeO_2H]^{2+}$ (goethite/limonite group of minerals)) + Ca-montmorillonite in some of the expelled ascending gas bubbles. (c) Detail of the sediment-water interface showing turbulent effect of micro-vent degassing. (d) Detail of the sediment (Fe^0 overlain by Ca-montmorillonite + $Fe_2O_3/Fe(OH)_x$) showing the close relationship between gas bubble formation and $Fe_2O_3/Fe(OH)_x$; width about 2 cm. The largest bubbles have diameter of 2-4 mm. Some ice/ice slush is present in the water column due to desalination associated with the presence of Fe^0 (Antia, 2010). Date 11/1/11.

During periods of pH decline and/or Eh decline, significant O_2(g) degassing (Antia, 2010) may accompany hydrocarbon formation (Fig. 6). Part of the O_2 discharge is associated with the formation of $Fe(OH)_x$ and Fe_2O_3 (Fig. 6).These observations suggest that methane formation is associated with increasing alkalinity while higher alkane formation is associated with decreasing Eh and/or decreasing pH.

3.4 Eh-pH Changes – Control Case

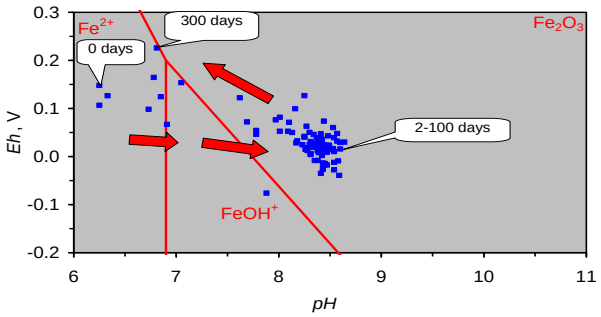

Fig. 7: Control Changes

In water Eh & pH associated with addition of 60 g/L Ca-montmorillonite at 263 – 298 K at 0.1 MPa in a sealed static diffusion reactor containing 0.2 L saline H_2O.

The control sample showed an initial minor increase in pH as the water adjusted to the presence of Al and Ca ions associated with the Ca-montmorillonite (Fig. 7). Over a period of 300 days the pH increase was reversed and the Eh increased (relative to the initial Eh). The final Eh was about 0.25 mV higher (Fig. 7) than in the base case containing Fe^0 (Fig. 5). Significantly no O_2(g), H_2(g) or CH_4/C_{1+}(g) bubbles (Fig. 6) were observed in the control reactor (Fig. 8).

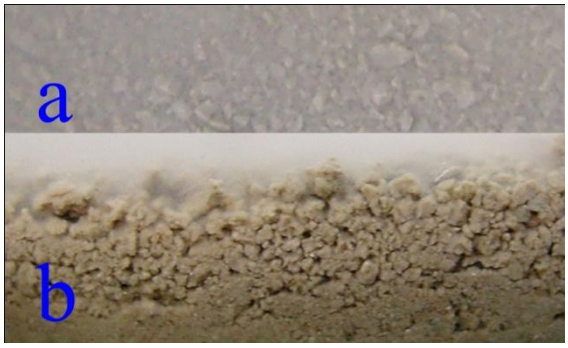

Fig. 8: Control Sample

60 g/L Ca-montmorillonite, 272 K at Day 300. (a) plan view through water to clay surface showing an absence of bubbles; width c.3 cm. (b) vertical section through the clay/water interface showing an absence of bubbles and a well developed network of clods and macropores at the clay/H_2O interface; width about 2 cm: Date 11/1/11.

4. EXPERIMENT Ⅱ

Experiment Ⅰ established that Fe^0 can catalyse the formation of light hydrocarbons at 0 – 30 C in an aqueous environment. However, most sedimentary sequences only contain minor concentrations of Fe, typically as Fe^{2+} ions, $FeOH^-$, Fe_2O_3 and $Fe[OH]_x$. These sequences may contain high concentrations of NaCl, either in solution or as halite. Halite, when combined with a zero valent metal (Fe^0 or Ni^0) will catalyse hydrocarbon formation from CO_2, CO and H_2(Gagnon, 2003; 2004; Antia, 2008b). Thermal and biogenic decomposition of organic matter releases CO_2 + CO + $C_xH_yO_z$ (formaldehydes, acetates) + HCO_3^- + CH_4 + H_2 (e.g. Verhaart *et al*. 2010). Experiment Ⅱ considers

whether NaCl is able to facilitate CO_2 removal from a flowing gas containing CH_4, and minor quantities of CO, H_2, H_2O, C_xH_y, $C_xH_yCl_z$ and $C_xH_yO_z$ produced by the thermal decomposition of organic matter at low temperatures.

4.1 Low Temperature Thermogenic Gas Composition

Low temperature (373-673 K) thermal decomposition of organic matter (in the presence of CO, CH_4, CO_2, O_2 or H_2O) produces a gas with a high CO_2:CO ratio and a high H_2O:H_2 ratio (Gaur & Reed, 1998). Prolonged heating periods result in almost complete gasification of the organic matter, leaving a residual char/ash. The rate of organic decomposition is accelerated by increasing temperature.

4.2 Reactor and Process Flow

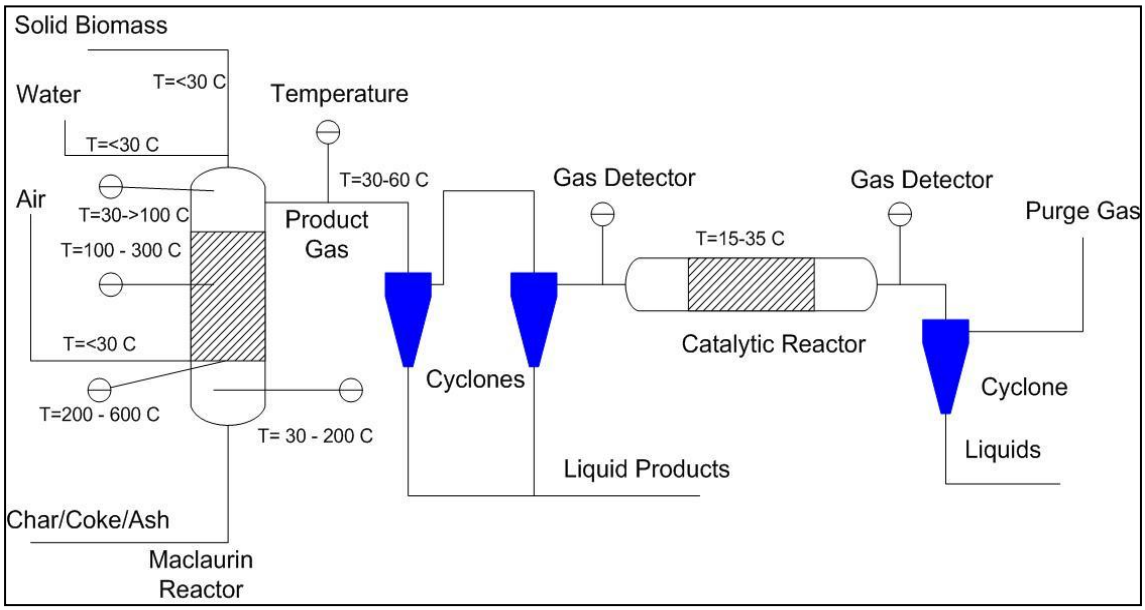

Fig. 9: Process Flow for Experiment Ⅱ

The thermogenic feed gas was constructed using a non-catalytic, internally heated, Maclaurin carbonisation reactor (Maclaurin, 1915) fed by angiosperm wood and foliage. The dominant gaseous products are H_2O, CO_2, CH_4, N_2, with minor quantities of CO, H_2, C_xH_y, $C_xH_yCl_z$ and $C_xH_yO_z$. Solid waste (char + ash) formed 10-30% by weight of the product. Entrained liquids and gaseous products (estimated effective reactor raw gas discharge rate = <0.10 – >60 $Nm^3\ hr^{-1}$) were passed through four cyclones/condensers, placed in series, to remove entrained and condensable liquids (Fig. 9). The residual gas (estimated 1 - 40% of raw gas volume) was passed through a packed bed reactor (0.06m internal diameter) containing 0.25 kg NaCl catalyst. The residual gas was passed through a cyclone/condenser, prior to purge. The CO_2 and CO content of the gas entering and leaving the catalyst bed was measured [Anton Telegan Sprint V1. Measurement limits: O_2 = 0-25%; CO_2 = 0-25%; CO – direct measurement = 0-0.1%, CO:CO_2 ratio measurement = 0 – 0.99 (for CO concentrations of 0.1 - 7%); T = -50-1100 C; Poole Instrument Calibration Ltd. Calibration Certificate No. 109406]. Measured O_2 readings were typically <0.2%. The process flow and associated flowline temperatures are summarised in Fig. 9. The solid feedstock is maintained at a temperature of <300 C for the bulk of its residence in the reactor.

4.3 NaCl Catalyst

Halite granules (Triassic, Cheshire) [0.5-5 mm diameter] are used as the catalyst, or were mixed (50 wt%) with Fe-montmorillonite or $FeSO_4$, or Mg_2SO_4, or K_2SO_4, or $CaCO_3$, or organic matter, or pyroclastics or ash (e.g. Fig. 10b,c,d,e). The halite contains, and is coated by, Fe_xO_y and $Fe_x[OH]_y$ (Figure 10c). Details of catalyst manufacture are provided elsewhere (Antia, 2008b).

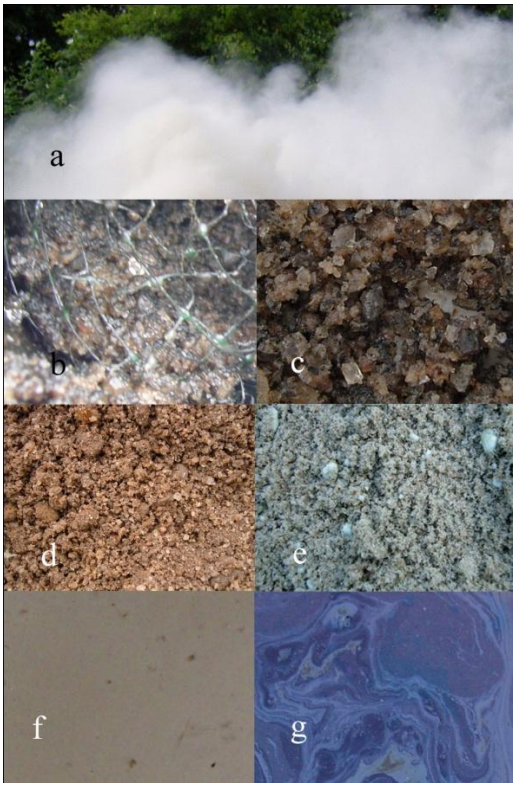

Fig. 10: Low Temperature Oil Formation

(a) Raw gas vented from the Maclaurin Reactor. (b) Halite catalyst in operation within the reactor showing H_2O formation on the catalyst surface. (c) Halite catalyst removed from the reactor contained bitumens; (d) Halite + Fe-montmorillonite catalyst; (e) Halite + Fe_2SO_4 catalyst. (f) solid alkanes produced by the halite catalyst. (g) liquid alkanes/hydrocarbons produced by the halite catalyst.

4.4 Test Results: Maclaurin Reactor

The Maclaurin reactor (Fig.9) produced a product gas (Fig. 10a) containing entrained particulates (H_2O, C_xH_y, $C_xH_yO_z$). The gas contained 1-20% CO_2 (Fig. 11). The cyclones (Fig. 9) recovered a number of different coloured organic compound-water mixtures (Fig. 12a-e) [toluene, alkyl acids, phenols, furains]. Aromatic crystals exsolved in the liquids during storage (Fig. 12a-e). Minor quantities of bitumen (Fig. 12f) and paraffinic wax (Fig. 12g) were produced. The gases leaving the downstream cyclone were essentially free of entrained particulates.

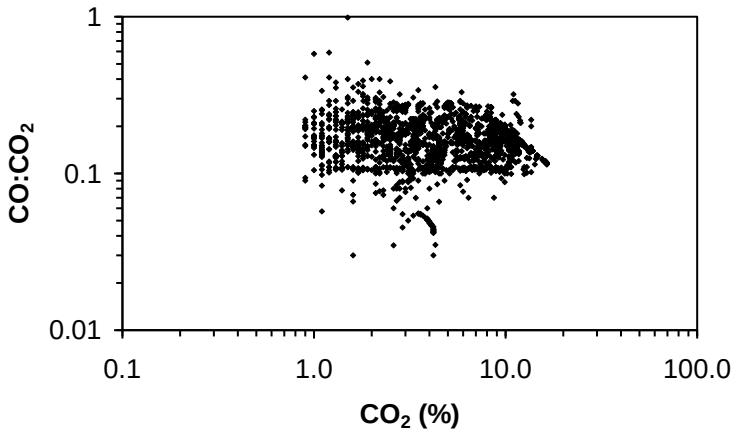

Fig. 11: CO_2 and CO Content of Product Gas from the Maclaurin Reactor

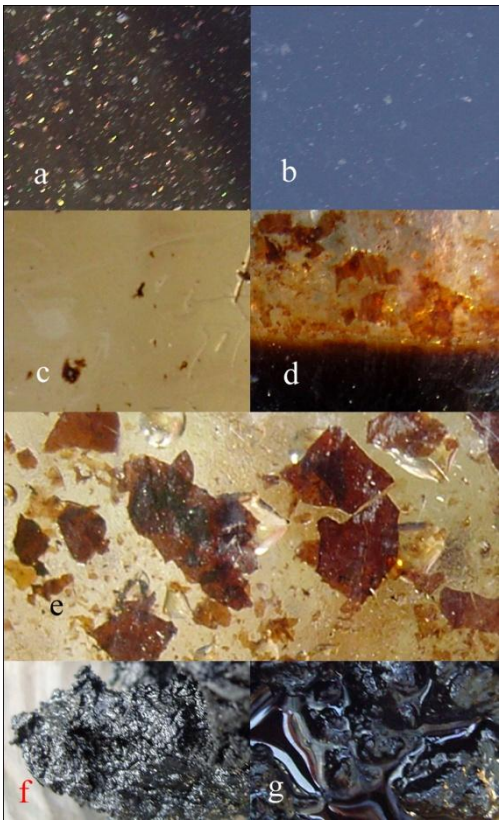

Fig. 12: Primary Products

From the Maclaurin Reactor. (a-c) Liquids (organic chemicals + water) containing crystallised aromatics. (d) Density separated liquid containing principally phenols + water overlain by water containing crystallised aromatics. (e) Examples of crystallised aromatics. Field of view = 3 cm. (f) Tar/bitumen, (g) Paraffinic waxes + aromatics.

4.5 Test Results: NaCl Packed Bed Reactor

It was observed that the passage of CO_2, CO through the catalyst bed (Fig.9; 10b,c,d) changed the molar abundance distributions [average (Fig. 13, 14, 15), standard deviation (Fig. 16), skewness (Fig. 17) and kurtosis (Fig.18)].

4.6 Interpretation of NaCl Test Results

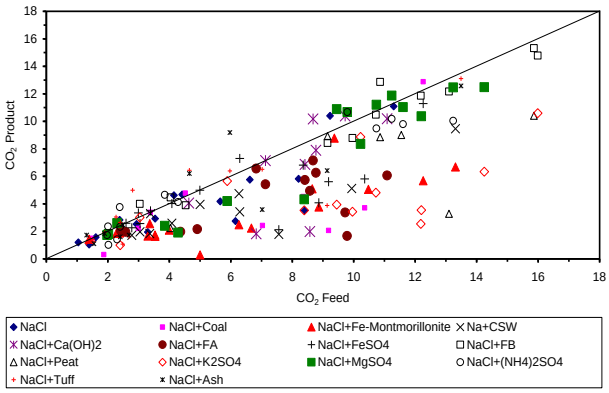

Fig. 13: Average Molar CO_2 Abundances (%) of Feed Gas and Product Gas

Number of Measurements = 8740. Analysis is not corrected for the decrease in product gas volume relative to feed gas volume. Temperature = 16 – 35 C; Pressure = 0.1 MPa.

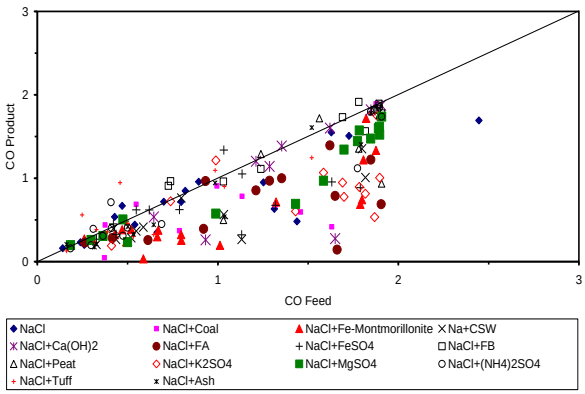

Fig. 14: Molar CO Abundances (%) of Feed Gas and Product Gas

CSW = nanoporous calcified algae skeletons; FA = organic rich nitrate fertiliser; FB = organic rich phosphate fertiliser; Ash = ash from the Maclaurin Reactor.

The molar abundances (Fig. 13, 14, 15) indicate that CO + CO_2 is removed from the feed gas within the catalyst bed. The feed gas discharge rate and feed gas composition from the Maclaurin reactor (Fig. 9) is in a state of constant flux (Fig. 11, 16-18). This variation creates a disequilibria within the catalyst bed. The surface of active NaCl catalyst within the catalytic reactor (Fig. 10b) is coated with product water. The solubility of CO_2 in this water is less than 0.03 M kg^{-1} (Duan and Sun, 2003) and is unlikely to account for >0.002 cm^3 CO_2. The CO_2 volumes removed are greater than the adsorption capacity of the NaCl (Saberi, 1996).

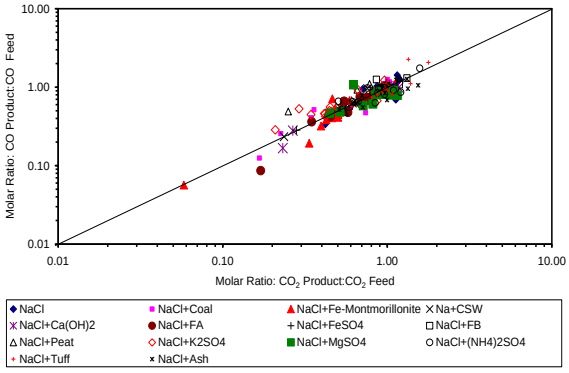

Fig. 15: Molar Product:Feed Ratios Assuming 1 Mole Feed Gas = 1 Mole Product Gas

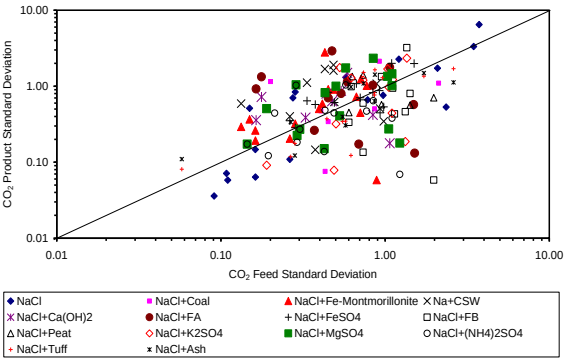

Fig. 16: Standard Deviation of Molar CO_2 Abundances of Feed Gas and Product Gas

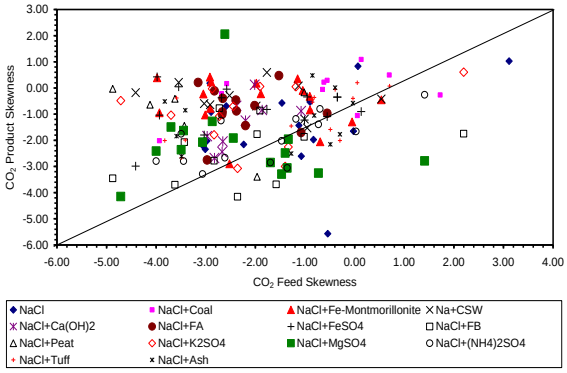

Fig. 17: Skewness Associated with Molar CO_2 Abundances of Feed Gas and Product Gas

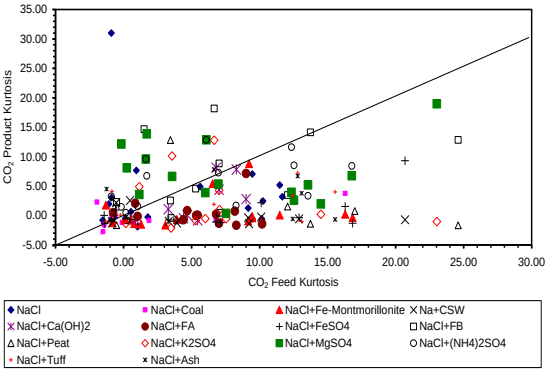

Fig. 18: Kurtosis Associated with Molar CO_2 Abundances of Feed Gas and Product Gas

The downstream collection cyclone (Fig. 9) contained a thin film of wax (Fig. 10f), minor quantities of oil (Fig. 10g) and no water. Bitumen was recorded within the spent catalyst (Fig. 10d). Fig. 1, 2 demonstrate that reaction E16 is both exothermic and spontaneous at atmospheric pressure and 298K. The observed water film on the NaCl (Fig. 10b) is interpreted as a reaction product (E16). The absence of water in the downstream cyclone (Fig. 9) is interpreted as indicating that any water produced via E16 is removed by reactions E1 to E10 (where Fe is substituted as appropriate by another cation).

$$C_eH_{2e+2} + bCO_2 + aCH_4 + cH_2 = C_nH_{2n+2} + dH_2O + fH_2;$$
$$n=e+a+b;\ H_2 = 2H_3O^+ \text{ or } 2H^+ \text{ or } 2Fe\text{-}H^+ \text{ or } Me\text{-}H^+ \qquad \text{(E16)}$$

5. CONCLUSIONS

The traditional oil formation model links hydrocarbon generation directly to the heating duration, heating rate and temperature of organic source rocks. It remains the most likely hydrocarbon generation model for most commercial oil and gas accumulations. However, most immature sediments (R_o=<0.6) at temperatures of 0 – 100 C contain extractable C_{5+} hydrocarbons and varying concentrations of C_1-C_5 gaseous hydrocarbons. While some of these hydrocarbons can be explained by migration from a deeper more mature source rock or formation as a result of microbial activity, the origin of the majority of these dispersed, low concentration, hydrocarbons is unknown.

Zero Valent Iron (ZVI) water treatment studies have demonstrated that alkane formation can be catalysed at <30 C using Fe^0 + water and a carbon source (Fig. 3, 4). 1 kg of C has the potential to produce a maximum of 1.8 m^3 CH_4. The reaction rates measured in Fig. 3 indicate that this ultimate potential (if the reactions run to completion) may naturally be achieved within a short time period (weeks to years). Experiment I established the Eh and pH associated with this hydrocarbon generation and possible reaction routes. This experiment established that anoxic alkaline pore water is more likely to catalyse methane formation, while anoxic neutral pore waters are more likely to catalyse the formation of C_{2+} hydrocarbons.

Hydrocarbon accumulations are commonly associated with saline pore waters and in some locations (e.g. Middle East, North Sea, Gulf of Mexico) with halite deposits (and halite diapers). Halites conventionally form part of a carbonate-evaporite sequence (of limestones, gypsum, halite and poly-halite). The associated oils and gases may have high H_2S concentrations (derived from gypsum) but commonly have very low CO_2 concentrations. Experiment II established that NaCl is able to facilitate the low temperature incorporation of CO_2 (within a migrating hydrocarbon gas) into longer chain hydrocarbon molecules (through Equations E1-E16) at <308 K. Experiment I has established that Fe^0, Fe_xO_y, $Fe(OH)_x$ minerals can catalyse the incorporationof CO_2 (and H_xCO_x) and H_2O into hydrocarbons at these temperatures (through Equations E1 –E12) under Eh and pH conditions which are common in many reservoirs (and hydrocarbon migration pathways). These observations may indicate that some of the dispersed C_{1-8+} hydrocarbons found in immature low temperature sediments (in the continental slope and abyssal plain) have an in situ catalytic origin, and may not indicate the presence of migrated hydrocarbons. The distribution of these low temperature hydrocarbons will be independent of sediment temperature, but may be directly linked to sediment facies/mineralogy and associated pore water chemistry.

REFERENCES

[1] Antia, D.D.J. (2008a). Oil polymerisation and fluid expulsion from low temperature, low maturity, over pressured sediments. *Journal of Petroleum Geology, 31*, 263 – 282.

[2] Antia, D.D.J. (2008b) *Ionic catalyst capture of carbon oxides*. GB Patent application GB2463878 A.

[3] Antia, D.D.J. (2009a). Low temperature oil polymerisation and hydrocarbon expulsion from continental shelf and continental slope sediments. *Indian Journal of Petroleum Geology, 16*(2), 1 – 30.

[4] Antia, D. D. J. (2009b).Polymerisation Theory – Formation of hydrocarbons in sedimentary strata (hydrates, clays, sandstones, carbonates, evaporites, volcanoclastics) from CH_4 and CO_2: Part I:Polymerisation concepts, kinetics, sources of hydrogen, and redox environment. *Indian Journal of Petroleum Geology, 17*(1), 49-86; Part II: Formation and Interpretation of Stage 1 to Stage 5 Oils, *Indian Journal of Petroleum Geology, 17*(2), 11-70; Part III: Hydrocarbon expulsion from the hydrodynamic flow regimes contained within a generating pressure mound. *Indian Journal of Petroleum Geology, 18*(1), 1-50.

[5] Antia, D.D.J. (2010). Sustainable zero-valent metal (ZVM) water treatment associated with infiltration, abstraction and recirculation. *Sustainability, 2*, 2988-3073.

[6] Antia, D.D.J. (2011). Modification of aquifer pore-water by static diffusion using nano-zero-valent metals.*Water, 3*, 79-112.

[7] Baxendale, J.H., Evans, M.G., & Kilham, J.K. (1946a). The kinetics of polymerisation reactions in aqueous solution. *Transaction Faraday Society, 42*, 668-675.

[8] Baxendale, J.H., Evans, M.G., & Park, G.S. (1946b). The mechanism and kinetics of the initiation of polymerisation by systems containing hydrogen peroxide. *Transaction Faraday Society, 42*, 155-169.

[9] Baxendale, J.H., Bywater, S., & Evans, M.G. (1946c). Relation between molecular weight and intrinsic viscosity for polymethyl methacrylate. *Journal Polymer Science, 1*, 237-244.

[10] Barbusinski, K. (2009). Fenton Reaction – controversy concerning the chemistry. *Ecological Chemistry Engineering, 16*, 347-358.

[11] Behar, B., & Stein, G. (1966). Photochemical evolution of oxygen from certain aqueous solutions. *Science, 154*, 1012-1013.

[12] Bokare, A.D., & Choi, W. (2009). Zero-valent aluminium for oxidative degradation of aqueous organic pollutants. *Environmental Science & Technology, 43*, 7130-7135.

[13] Braun, D. (2009). Origins and development of initiation of free radical polymerisation process. *International Journal of Polymer Science.* Article ID 893234, 10 p.

[14] Campbell, T.J., Burris, D.R., Roberts, A.L., & Wells, J.R. (1997). Trichloroethylene and tetrachloroethylene reduction in a metallic iron-water-vapor batch system. *Environmental Toxicology Chemistry, 16,* 625-630.

[15] Deng, B., Cambell, T.J., & Burris, D.R. (1997). Hydrocarbon formation in metallic iron/water systems. *Environmental Science & Technology, 31,* 1185-1190.

[16] Deng, B., Burris, D.R., & Campbell, T.J. (1999). Reduction of vinyl chloride in metallic iron-water systems. *Environmental Science & Technology, 33,* 2651-2656.

[17] Duan, Z., & Sun, R. (2003). An improved model calculating CO_2 solubility in pure water and aqueous NaCl solutions from 273-533 K and from 0 to 2000 bar. *Chemical Geology, 193,* 257-271.

[18] Elworthy, H.S., &Williamson, E.H. (1902). *Manufacture of gas consisting chiefly of methane or marsh gas for illuminating, heating and power purposes*. GB Patent 12,461, 31 May, 1902.

[19] Evans, M.G., George, P., & Uri, N. (1949). The $[Fe(OH)]^{+2}$ and $[Fe(O_2H)]^{+2}$ complexes. *Transaction Faraday Society*, *45*, 230-36.

[20] Gagnon, R. (2003).*How to convert carbon monoxide into synthetic petroleum by a process of catalytic CO petrolisation.* US Patent 6774149.

[21] Gagnon, R. (2004).*How to convert carbon dioxide into synthetic hydrocarbon through a process of catalytic hydrogenation called CO_2 hydrocarbonation.* US Patent 6987134.

[22] Gaur, S., & Reed, T.B. (1998). *Thermal data for natural and synthetic fuels*. New York: Marcel Dekker.

[23] George, P. (1952). The specific reaction of iron in some Hemoproteins. In.W.G. Frankenburg (ed.) *Advances in Catalysis and related subjects, IV,* 367-428. New York: Academic Press.

[24] Hardy, L.I., Gillham, R.W. (1995). Formation of Hydrocarbons from the reduction of aqueous CO_2 by zero valentiron. *Environmental Science & Technology, 30,* 57-65.

[25] Hori, Y., Murata, A., & Takahashi, R. (1989). Formation of hydrocarbons in the electrochemical reduction of carbon dioxide at a copper electrode in aqueous solution. *Journal Chemical Society Faraday Transactions, 85,* 2309-2326.

[26] Kang, S-H., Choi, W. (2009). Oxidative degradation of organic compounds using zero-valent iron in the presence of natural organic matter serving as an electron shuttle. *Environmental Science & Technology, 43*, 878-883.

[27] Kolbel, H.; Engelhardt, F., (1959). *Synthesis of hydrocarbons and oxygen-containing organic compounds*. US Patent US2917531.

[28] Kotz, J.C., & Treichel, P. (1996). *Chemistry & Chemical Reactivity*. Fort Worth, Saunders College Publishing.

[29] Kuster, H. (1936a). Reduction of carbon dioxide to higher hydrocarbons at atmospheric pressures by catalysts of the iron group. *Brennstoff-Chem, 17,* 221-228.

[30] Kuster, H. (1936b). Reduction of carbon dioxide to methane upon iron catalysts at ordinary pressures. *Brennstoff-Chem, 17,* 203-206.

[31] Lim, T-T., Feng, J., & Zhu, B-W. (2007). Kinetic and mechanistyic examinations of reductive transformation pathways of brominated methanes with nano-scale Fe and Ni/Fe particles. *Water Research, 41,* 875-883.

[32] Maclaurin, R. (1915). *Manufacture of various products from bituminous fuel*. US Patent 1,130,001.

[33] Mwebi, N.O. (2005). *Fenton & Fenton-like reactions: the nature of oxidizing intermediates involved* (Ph.D Thesis). University of Maryland, USA.

[34] O'Rear, D.J. (2005). *Conversion of syngas to distillate fuels.* US Patent US6864398.

[35] Puskas, I. (1997). Can carbon dioxide be reduced to high molecular weight hydrocarbons? *Proceedings American Chemical Society, ACS 213* National meeting (San Fransisco, Apr. 13-17 1997). Retrieved from http: www.anl.gov/PCS/acsfuel/preprint%20archive/Files/42_2_SAN% 20FRANSICO_04-97_0680.pdf

[36] Sabatier, P. (1908). *Manufacture of methane or mixtures of methane and hydrogen*. French Patent 400656.

[37] Sabatier, P. (1910). *Process of manufacturing methane or of mixtures of methane and hydrogen.* US Patent US00956734.

[38] Saberi, M-A. (1996). The structure of carbon dioxide adsorbed on a sodium chloride (001) surface (Master's Thesis). Concordia University, Montreal, Canada.

[39] Schrick, B., Blough, J.L., Jones, A.D., & Mallouk, T.E. (2002). Hydrochlorination of trichloroethylene to hydrocarbons using bimetallic nickel-iron nanoparticles. *Chemical Materials, 14*, 5140-5147.

[40] Steynberg, A., &Dry, M. (2004). *Fischer-Tropsch Technology*. New York: Elsevier.

[41] Storch, H.H., Golumbic, N., & Anderson, R.B. (1951). *The Fischer-Tropsch and related synthesis.* New York: Wiley.

[42] Verhaart, M.R.A., Bielen, A.A.M., van der Oost, J., Stams, A.J.M., & Kengen, S.W.M. (2010). Hydrogen production by hyperthermophillic bacteria and archaea: mechanisms for reductant disposal. *Environmental Technology, 31*, 993-1003.